HCl, KCl and KOH Solvation Resolved Solute-Solvent Interactions and Solution Surface Stress

Xi Zhang[*,†], Yan Xu[‡], Yong Zhou*, Yinyan Gong[‡], Yongli Huang[§], Chang Q Sun*[,**]

Abstract

An incorporation of the hydrogen bond (O:H-O or HB) cooperativity notion, contact angle detection, and the differential phonon spectrometrics (DPS) has enabled us to gain refined information on the HCl, KCl and KOH solvation resolved solute-solvent molecular interactions and the solution surface stresses. Results show that ionic polarization stiffens the solvent H-O bond phonon from 3200 to 3480 cm^{-1} in the hydration shells. The HO^- in alkaline solution, however, shares not only the same H-O phonon redshift of compressed water from 3200 to < 3100 cm^{-1} but also the dangling bonds of H_2O surface featured at 3610 cm^{-1}. Salt and alkaline solvation enhances the solution surface stress by K^+ and Cl^- ionic polarization. The excessive H^+ proton in acid solution forms a H↔H anti-HB that depresses the solution surface stress, instead. The solute capability of transforming the fraction of the O:H-O bonds of the solvent matrix is featured by: $f_H = 0$ and $f_x \propto 1\text{-}\exp(-C/C_0)$ (x = HO^-, K^+ and Cl^-) towards saturation. Exercises not only confirm the presence of the H↔H anti-HB point fragilization, the O:⇔:O super-HB point compression, and ionic polarization dominating the performance of the respective HCl, KOH, and KCl solutions, but also demonstrate the power of the DPS that enables high resolution of solute-solute-solvent interactions and correlation between HB relaxation and solution surface stress.

Keywords: Hydrogen bond; interface; electrolyte; surface stress

[*] Key Laboratory of Extraordinary Coordination Bond and Advanced Materials Techniques (EBEAM) of Chongqing, Yangtze Normal University, Chongqing 408100

[†] Institute of Nanosurface Science and Engineering, Shenzhen University, Shenzhen 518060, China; (Zh0005xi@szu.edu.cn)

[‡] Institute of Coordination Bond Metrology and Engineering, College of Materials Science and Engineering, China Jiliang University, Hangzhou 310018, China

[§] Key Laboratory of Low-Dimensional Materials and Application Technologies (Ministry of Education) and School of Materials, Science and Engineering, Xiangtan University, Hunan 411105, China

[**] Nanyang Technological University, Singapore 639798, Singapore; (ecqsun@ntu.edu.sg)

Highlight

- Acid solvation derives H↔H point breakers that disrupt the solution surface stress
- Base solvation derives O:⇔:O point compressors sharing the same effect of pressure
- Electric fields of aqueous Ions cluster, stretch and polarize the hydrogen bond
- DPS resolves solute capabilities of transforming the solute-solvent interface bonds

Content entry

DPS distils information on transforming the stiffness (frequency shift), fraction (peak area) and fluctuation (FWHM) of H-O bonds upon HCl, HOH and KCl solvation, which suggests the essentiality of H↔H anti-HB fragilization, O:⇔:O super-HB compression, and K^+ + Cl^- polarization in solutions.

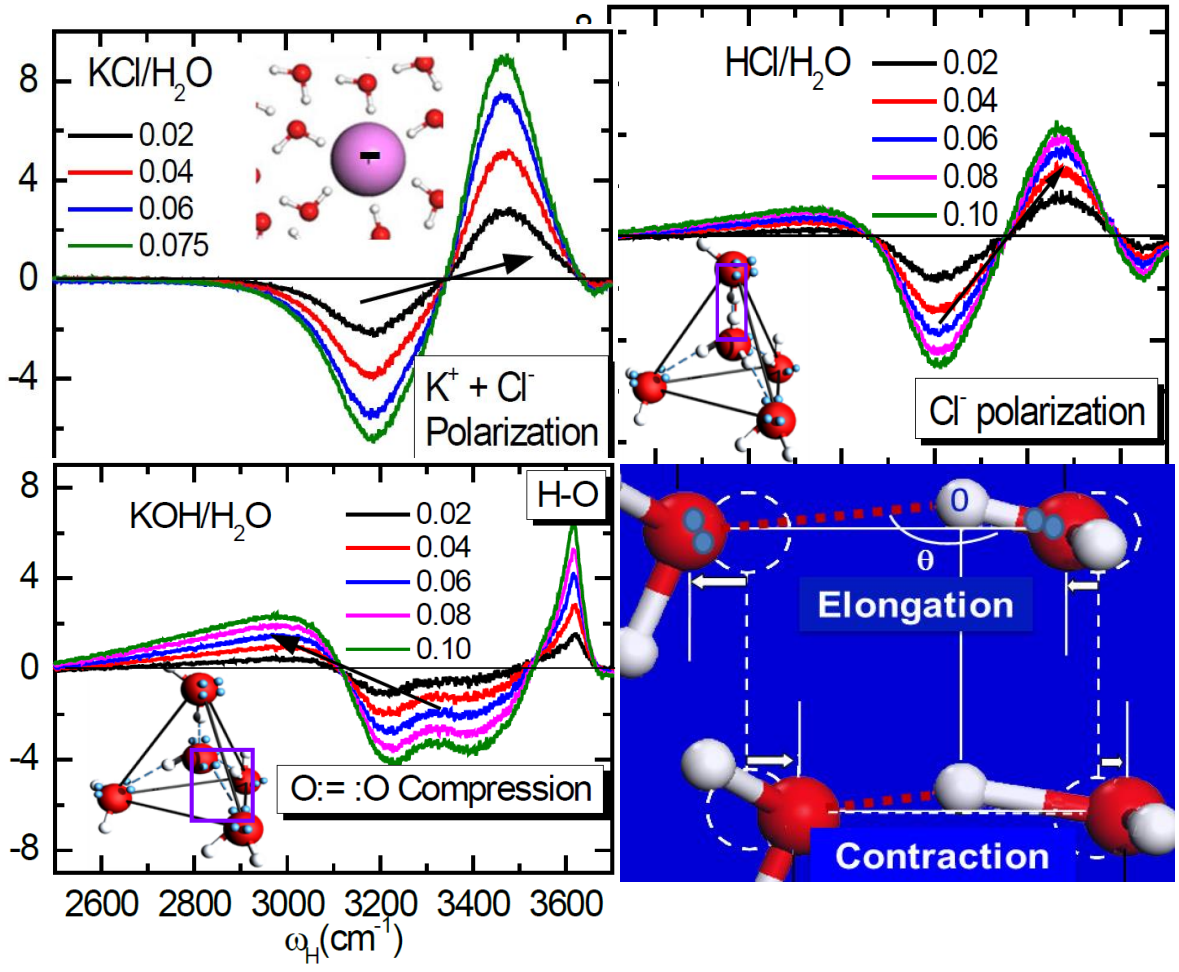

1. Introduction

As functional groups, solvation of acid, base, and salt is ubiquitously important to modulating cell activities and solution surface stress [1-7]. However, high resolution and clarification of solute-solute-solvent molecular interactions and correlation to the solution surface stress remain yet high challenge, though the acid-base-adduct dissolution has been well defined century-long ago [8-11] in terms of H^+ and OH^- donation or by means of electron pair acceptance and donation. Intensive spectroscopic investigations have been conducted on the dynamics of acid-base-salt hydration for decades. For instances, the sum frequency generation (SFG) spectroscopy provides information on the sublayer-resolved dipole orientation, or the skin dielectrics, at the air-solution interface [12, 13], while the ultrafast two-dimensional infrared absorption (t-2DFR) probes the solute or water molecular diffusion dynamics in terms of phonon lifetime and the viscosity of the solutions [14, 15].

Salts solutions demonstrate the Hofmeister effect [1, 16] on regulating the skin stress and the solubility of proteins with possible mechanisms of structural maker and structural breaker [17-19], ionic specification [20, 21], quantum dispersion [20] and skin induction [22]. Quantum modulation of hydrogen bond is also important in ligand-water interaction [23] and cellobiose-water interactions [24]. Observations revealed that 1 M salt of KX (X = I, Br, Cl, and F) hydration [25] raises the H-O stretching vibration frequency (ω_H) in the Hofmeister series order [16, 26] - larger ions of less electronegative stiffen the ω_H more significantly [27, 28]. Molecular dynamics (MD) simulations and t-2DIR measurements [29] unveiled that an addition of 5% NaBr to the HOD/H_2O solution raises the O-D vibration wavenumber from ~2509 to ~2539 cm^{-1} and the amount of shift changes with the H_2O/Br^- molecular ratio (varying from 8, 16, to 32). The anion interaction with water molecules prolongs the lifetime of molecular dynamics [30], indicating the viscosity enhancement of the solution. Salt hydration shifts the H-O peak from 3200 to 3450 cm^{-1} and narrows the H-O peak, which indicates the slow molecular translational and vibrational motion that is proportional inversely to the linewidth of the characteristic phonon spectral peak [26].

The mobility of the excessive H^+ proton in acid solutions was explained in terms of "structural diffusion" [31] with involvement of thermal hopping [32], proton tunneling [33] or fluctuating [34]. In 1960s, Eigen [35] proposed an $H_9O_4^+$ complex in which an H_3O^+ core is strongly hydrogen-bonded to three H_2O molecules and leave the lone pair of the H_3O^+ free. Zundel [36] favors the notion of an $H_5O_2^+$ complex in which the proton is shuttling freely between two H_2O molecules. Using the *ab initio* path integral simulations, Marx et al [37] noted that the hydrated proton forms a fluxional defect in the hydrogen-bonded network, with both $H_9O_4^+$ and $H_5O_2^+$ occurring only in the sense of 'limiting' or 'ideal' structures. The defect can become delocalized over several hydrogen bonds owing to quantum fluctuations. A computational study [38] suggested that protons transfer collectively in ice and the manner of motion varies with temperature and the thermal and quantum fluctuations are involved.

Studies of NaOH base hydration in bulk water [39] and in water clusters [40] revealed two processes of vibration relaxations. One is the rapid process on 200 ± 50 fs time scales (corresponds to the slow H-O bond vibration) and the other slower dynamics on 1–2 ps scales (fast H-O bond vibration) [15]. The fast and the slow processes are being understood as due the compression elongated solvent H-O bond and the fast one due the HO^- solute H-O bond [41], as discussed subsequently. The vibrational energy exchange between the bulk-like water and the hydroxide-associated water takes place in ~200 fs. The strong nonlinear coupling between intra- and inter-molecular vibrations and the non-adiabatic vibrational relaxation could be responsible for the rapid dynamics of phonon relaxation. An addition of 7M NaOH could fold the slower decay time or increases four-fold the viscosity of pure water. Meanwhile, the IR spectra undergo a broadening or a redshift with transition of the abundance from above 3000 cm^{-1} to its below. The free and the hydrogen bonded OH^- stretching of the $OH^-(H_2O)_{4,5}$ cluster broadens the phonon band substantially [42].

For aqueous chloride, bromide and iodide, higher solute concentration shifts more the H-O band to the blue [26, 43], while for hydroxide (base) the H-O vibration mode shifts to lower frequencies. These spectral changes are usually explained as Cl^-, Br^-, and I^- ions weakening of the surrounding H-bond (structure breakers) or OH^- strengthening of the H-bonging (structure makers). Unfortunately, little

attention has been paid to the network O:H-O bond cooperative relaxation induced by acid-base-salt solvation. It is yet poorly known how the H^+, OH^-, Y^+ and X^- ions interact with water molecules of the hydration networks and how the ions relax the hydrogen bond (HB, or O:H-O with ":" being electron lone pair of oxygen) in the hydration shells, until the recent progresses made by this group [27, 28, 41, 43, 44]. In fact, knowledge lacking about the structure of the liquid water and the relaxation dynamics of the HB [45] has prevented largely the progress in understanding the solute-solvent-functionality in aqueous solutions.

2. Principles

2.1 Phonon relaxation spectrometrics

A Raman spectral peak features the Fourier transformation of all bonds vibrating in the same frequency from the real space, irrespective of their locations or orientations in the liquid, solid, or vapor phase of the same substance. One can only probe the statistic mean of the vibrations and its fluctuation but cannot resolve the source of stimuli. The spectral peak frequencies correspond to the respective bond stiffness [46]. Raman phonon frequency shift $\Delta\omega_x$ probes, in the first order approximation, the stiffness of O:H and H-O bonds relaxes cooperatively as a function of the segmental length d_x and energy E_x,[47]

$$\Delta\omega_x \propto \sqrt{E_x/\mu_x}\,/\,d_x \propto \sqrt{(k_x + k_c)/\mu_x} \tag{1}$$

The subscript x = L denotes the O:H nonbond characterized by the stretching vibration frequency at ~200 cm^{-1} and x = H denotes the H-O bond with characteristic phonon frequency of ~3200 cm^{-1} in the bulk water. The k_x and k_C are the force constants or the second differentials of the intra/inter molecular interaction and O-O Coulomb coupling potentials. The $\Delta\omega_x$ also varies with the reduced mass μ_x of the specific x oscillator. However, from the full-frequency Raman spectra, one could hardly be able to gain quantitative information on the transformation of the stiffness, fraction, and fluctuation of bonds being functionalized by solvation.

Compared with the convention of Gaussian fitting, differential phonon spectrometrics (DPS)[48, 49]

distills the characteristic phonons by differencing the spectra collected before and after conditioning, which distils transformation of the stiffness (frequency shift), fraction (peak area) and fluctuation (linewidth) of the H-O bonds being conditioned upon solute solvation, mechanical compression, thermal excitation, molecular undercoordination, etc. Figure 1c and d exemplify the DPS measured under mechanical compression of liquid water and skin molecular undercoordination of water and ice. External compression softens the H-O phonon but bond order deficiency stiffens the ω_H for the supersolid skin of liquid water and ice.[47] Therefore, DPS resolves unambiguously the effect of conditioning on the O:H-O bond cooperative relaxation and structural transition in a solution [50].

2.2 Hydrogen bond relaxation

As illustrated in Figure 1, as a strongly correlated and fluctuating system, water prefers the statistic mean of the tetrahedrally-coordinated, two-phase structure in a bulk-skin or a core-shell order of different O:H-O bond lengths [46, 51]. Representing the entire periodic HB network of water, the alkaline $2H_2O$ unit cell contains four oriented HBs (Figure 1a). The O:H-O bond consists the weaker O:H intermolecular (~0.1 eV) and the stronger H-O intramolecular (~4.0 eV) short-range interactions and the Coulomb repulsion between electron pairs on adjacent oxygen ions [52]. The HB is universal to water and ice irrespective of its phase structure, even though the ionic H_3O^+:OH^- phase (at 2 TPa pressure and 2000 K temperature) [53], the symmetrical ice-X phase of identical O:H and H-O lengths (at 60 GPa over all temperatures) [47, 54], and solvent matrix of the aqueous solutions.

The O:H nonbond and the H-O bond segmental disparity and the O-O coupling allow the segmented O:H-O bond to relax oppositely – an external stimulus dislocates both O ions in the same direction but by different amounts (Figure 1b). The softer O:H nonbond always relaxes more than the stiffer H-O bond with respect to the H^+ coordination origin. The ∠O:H-O containing angle θ relaxation contributes only to the geometry and mass density [28]. There are only two ways of O:H-O bond relaxation – elongation or contraction. Liquid heating and bond order deficiency lengthen the O:H-O bond associated with charge polarization and depolarization but compression shortens it with polarization [47]. Furthermore, one segment of the HB will be stiffer if it becomes shorter, and its characteristic frequency undergoes a blue shift; the other segment will react cooperatively and

oppositely.

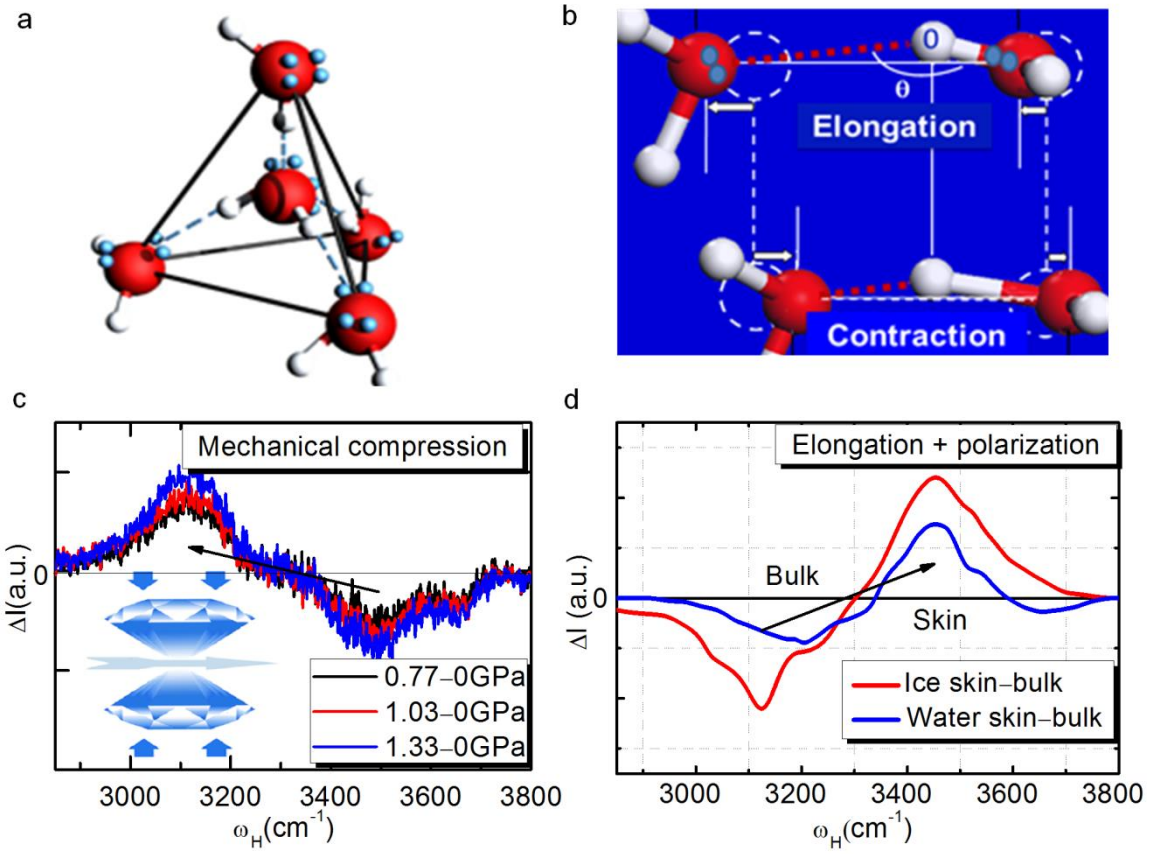

Figure 1. (a) Water structure and the (b) cooperative relaxation of the segmented O:H-O bond. The pairing dots represent the nonbonding lone pairs on oxygen. (c) H-O phonon frequency shift of 25°C water under different pressures. Inset shows the schematic diagram of mechanical compression. (d) The differential Raman spectra between skin and bulk of 25°C water and of –20°C ice. Compression lengthens and softens the H-O bond but the skin bond-order deficiency shortens and stiffens the H-O bond.[55]

The O:H nonbond and the H-O bond segmental disparity and the O-O coupling allow the segmented O:H-O bond to relax oppositely – an external stimulus dislocates both O ions in the same direction but by different amounts (Figure 1b). The softer O:H nonbond always relaxes more than the stiffer H-O bond with respect to the H^+ coordination origin. The ∠O:H-O containing angle θ relaxation contributes only to the geometry and mass density [28]. There are only two ways of O:H-O bond

relaxation – elongation or contraction. Liquid heating and bond order deficiency lengthen the O:H-O bond associated with charge polarization and depolarization but compression shortens it with polarization [47]. Furthermore, one segment of the HB will be stiffer if it becomes shorter, and its characteristic frequency undergoes a blue shift; the other segment will react cooperatively and oppositely.

The Raman spectra of compressed water, shown in Figure 1c, were measured in a symmetric diamond anvil cell (DAC)[43]. The cell consists of two culet diamonds with a face of 1000 μm in diameter. Deionized water was placed between them for measurement. In-situ Raman spectroscopy was was conducted when the pressure varied. Figure 1d shows the $\Delta\omega_H$ of 25 °C water and ice (at -20 and -15 °C) [56]. The $\Delta\omega_H$ is the difference between two spectra collected at different angles between the scattered light and the sample's surface normal. Water and ice skins share an identical ω_H of 3450 cm^{-1} shifting from the bulk water at 3200 cm^{-1} and bulk ice at 3150 cm^{-1}. An integration of the peak at 3450 cm^{-1} estimates that the skin of the ice is 9/5 thicker than the water because the skin molecular thermal fluctuation.

For the undercoordinated $(H_2O)_n$ clusters, scanning tunneling microscopy at extremely low temperatures and ultra-high vacuum has probed concerted proton quantum tunneling occurs to tetramer by rotation [57]; computations suggested that protons transfer collectively in ice driven by thermal and quantum fluctuations [38]. Nuclear quantum effect also plays an important role in relaxing the hydrogen bond at high vacuum and low temperatures [58]. The proton behavior under these extreme conditions, low molecular coordination, low temperature, and high vacuum provides better understanding of the performance of liquid water and would be helpful to the understanding of the acid, base, salt solvation dynamics.

2.3 Solute quantum modulation

In place of the conventional focus of solute motion dynamics, we examined the solute capabilities of transforming the stiffness, fluctuation, and abundance of the bonds of the solution, in particular, the HBs in the first hydration shells, as the DPS distills only the most pronounced transition of the

phonons. As illustrated in Table 1 and Figure 2, an H_2O molecule has two negative lone electron pairs and two protons interaction with either a lone pair or a proton of the neighboring H_2O molecule. From the number of lone pairs and protons wise, H_2O is neutral and harmonious. Therefore, one can observe the performance and the capabilities of a solute from the perspective of number harmonicity of the negative lone pairs and the positive protons, and spatial symmetry of distributions in particular for solvation of complex solutes.

A HX acid molecule dissolves into the H^+ and the X^- and a YOH base into a Y^+ and an OH^- hydroxide. The X^- and Y^+ remain isolated in solutions but the H^+ bonds immediately to one H_2O to form a H_3O^+ hydronium. Both the H_3O^+ and the OH^- retain the tetrahedron structure of H_2O but the H_3O^+ has an excessive H-O bond and the OH^- has an additional lone pair.

A H_3O^+ and OH^- substitution for the central H_2O molecule in the $2H_2O$ unit cell creates regularly the (a) H↔H anti-HB point breaker and (b) the O:⇔:O super-HB point compressor. These point switchers govern the performance of the hydration network of acid, base, and salt solutions. The relative number of such unit cells in the solution is proportional to the solute molar concentration. The ions in all solutions serve as each a point polarizer that aligns, stretches, and polarizes the surrounding hydrogen bonds to form their hydration shells. The H↔H anti-HB disrupts the solution network and the surface stress [44]. The O:⇔:O super-HB compresses the neighboring O:H-O bond [41]to have the same effect of mechanical compression that shortens the O:H distance and elongate the H-O bond [43].

Table 1 Quantum point switchers for the HCl, KCl, and KOH solute-solvent-functionality.

Solution			Hydration dynamics	Functionality
HCl (Acid)	HCl + $H_2\ddot{O}$:	⇉	$Cl^- + H_3\ddot{O}^+$ ($H^+ \leftrightarrow H^+$ anti-HB point breaker)	Anti-HBs fragilization, embrittlement, corrosive, dilutive, skin stress destructive, etc.
KCl (Salt)	KCl + $H_2\ddot{O}$:		$Cl^- + K^+ + H_2\ddot{O}$: (Cl^- and K^+ point polarizer)	Ionic point polarizers align, polarize, and stretch the HBs. Skin stress constructive; thermally more stable; protein solubility; supersolidity; etc.
KOH (Base)	KHO + $H_2\ddot{O}$:		$H\ddot{O}:^- + K^+ + H_2\ddot{O}$: (O:⇔:O super-HB point compressor)	Super-HB makes the neighboring O:H-O bond shorter. Solution greasiness; burning heat, skin stress constructive, etc.

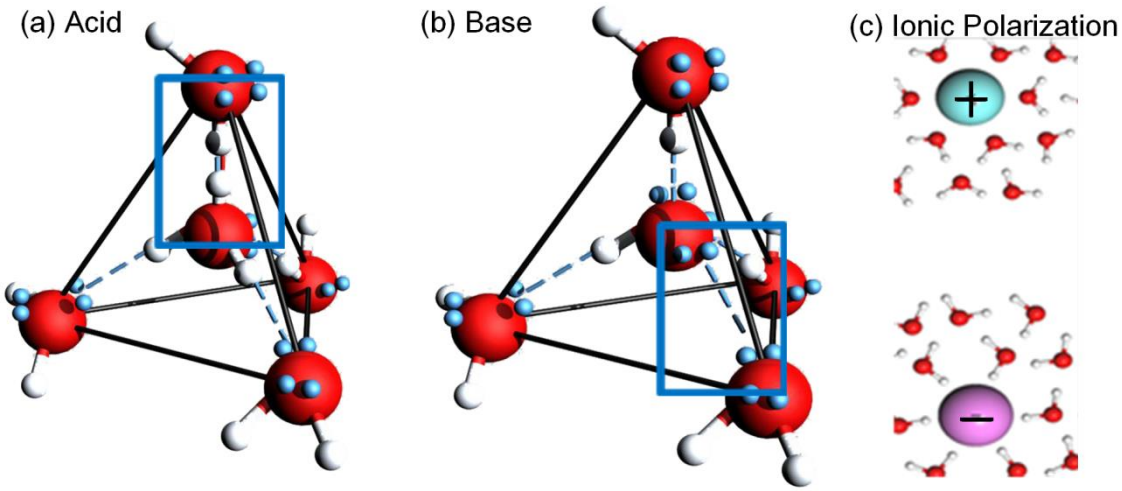

Figure 2. Illustration of the molecular structures of acid, base, and salt solutions. Framed are (a) the H↔H anti-HB point breaker and (b) the O:⇔:O super-HB point compressor. Ions in (c) serve each as a point polarizer that aligns, stretches and polarizes the O:H-O bond between oxygen ions.

3. Results and Discussion

3.1 Raman spectra and contact angle

With the aid of the Raman spectrometrics and contact angle measurements, as shown in Figure 3, we can resolve the phonon response to the point switchers on the performance of the HB networks and the associated properties with focusing on the HCl, KOH and KCl solutions. Indeed, KCl and HCL solutes have the same effect of bond order deficiency on the H-O bond relaxation (see inset a[47]) to form the supersolid hydration shells of stiffer H-O bond but different phonon abundances. KCl and KOH addition raises the skin stress but the HCl acid addition depresses the stress, which is general to other salt and acid solutions.[3]

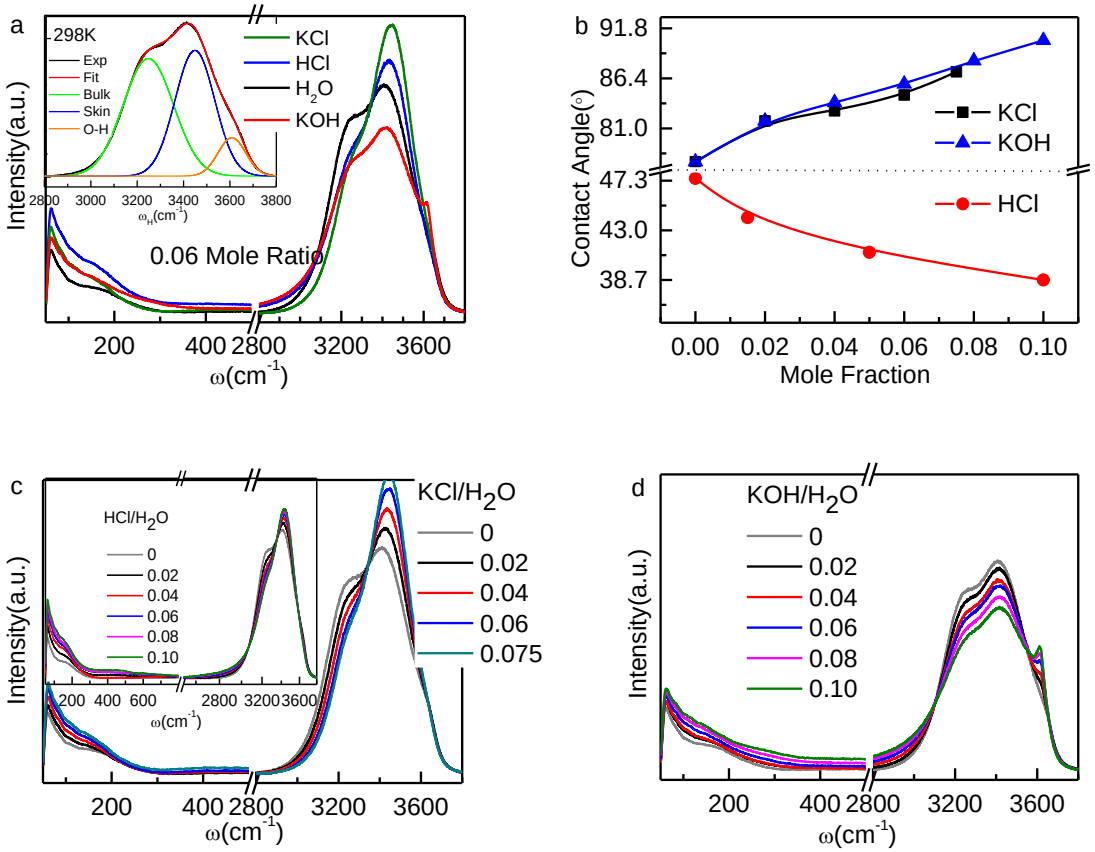

Figure 3. (a) Phonon frequency and (b) contact angle response to the solute type, KCl, HCl and KOH, of 0.06 mole fraction. The inset (a) shows the H-O phonon components of the bulk (3200 cm^{-1}), skin (3450 cm^{-1}), and the H-O free radical (3610 cm^{-1}) components for pure water. Features below 200 cm^{-1} characterizes the O:H nonbond stretching vibration. Phonon frequency of (c) KCl, inset (c) HCl

and (d) KOH with different concentrations in mole fraction.

3.2 DPS derivatives

Figure 4a and b show that HCl and KCl solvation does indeed softens the O:H nonbond by redshifting its ω_L from 200 to 100 cm^{-1}, and stiffens the H-O bond by blueshifting the ω_H from 3200 cm^{-1} to 3480 cm^{-1}. The cooperative shifts of the ω_L and the ω_H arises from stretching of the O:H-O bond and weakening the O-O repulsion. The O:H-O bond relaxation in length and stiffness due to polarization is the same to molecular undercoordination of skins of ice and water (see Figure 1d). Therefore, the hydration shell is like the water skin, behaving supersolidity, where supersolid means highly-ordered structure (longer ω_H lifetime[15]), high stress, polarized charge distribution, low density, and high thermal stability [28, 47]. The supersolid hydration shell dictates the Hofmeister effect of salt solutions in regulating the surface stress and make the proteins soluble [6, 7].

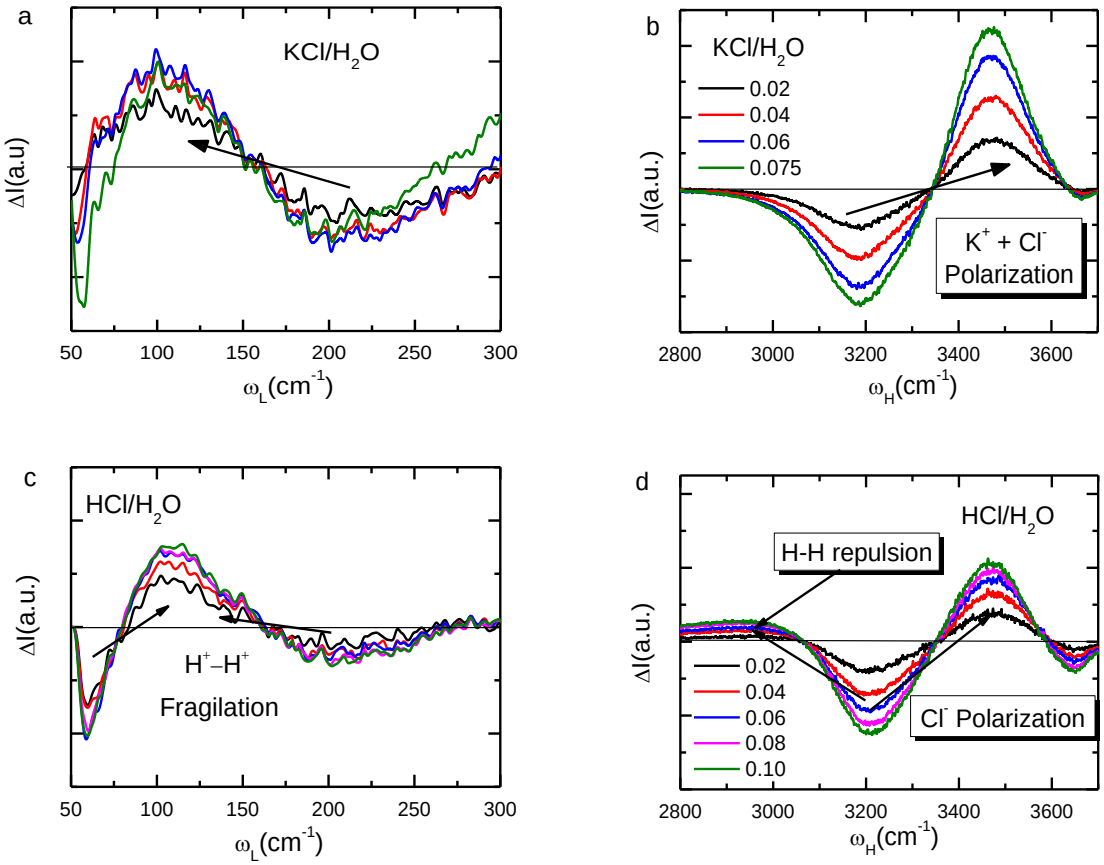

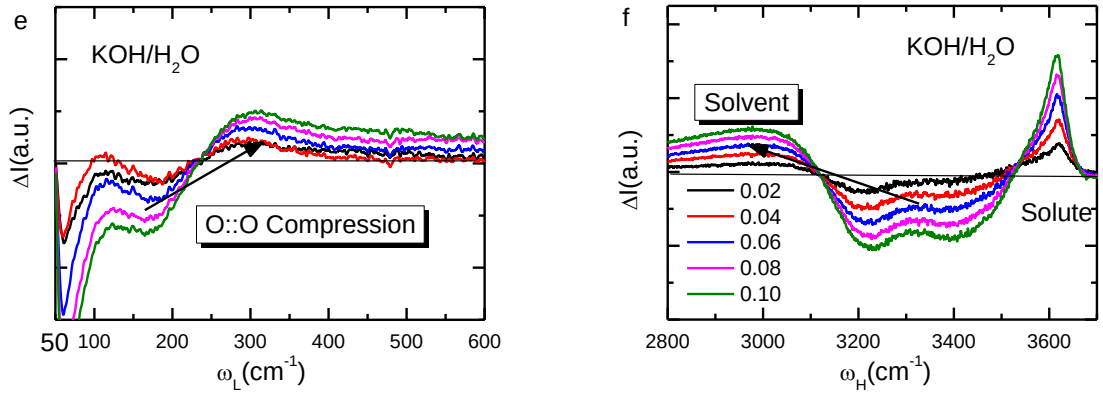

Figure 4. DPS of O:H and H-O phonon frequency and abundance response to the (a, b) quantum polarization in KCl (saturates at 0.075 mole fraction), (c, d) quantum fragilization in HCl, and (e, f) quantum compression in KOH solutions as a function of mole fraction concentration. Insets illustrate the respective unit cell obtained by replacing the central $H_2Ö$: molecule with +/- ions, a hydronium $(H_3O:)^+$, and a hydroxide $(H:Ö:)^-$.

However, a comparison of the ω_H phonon abundance for the KCl and the HCl solution in Figure 4b and d confirmed that the H^+ in the HCl solution does not stand-alone to polarize its neighbouring HBs but bonds to a H_2O to form H_3O^+ firmly. The H_3O^+-center unit has three H-O bonds and one lone pair (inset b circled), which is equivalent to form the $H_{2n+1}O_n^+$ clusters with n = 2 and 4 in the solution.[37] The H↔H is namely the anti-HB. The anti-HB pin holes the water network regularly, fragilating the HB network like its embrittlement in metals and alloys.[59, 60] This point fragilization is responsible for the corrosion ability of acid solutions. The Cl^- polarizer in the acid solution forms the hydration shell, which compensates the H↔H repulsion effect on the O:H phonon relaxation dynamics. Therefore, the electrostatic interaction of Cl^- shifts the ω_H to 3480 cm^{-1} with lesser abundance than that of the KCl solution of the same concentration and the H↔H repulsion recovers the ω_L from 100 to 110 cm^{-1}, as shown in Figure 4c and d. The fast occurrence of protons concerted quantum tunneling and quantum fluctuation [38, 57, 58] in ice clusters at extreme conditions is out of the current DPS scope that proves statistic information on hydrogen bond relaxation under the ambient condition upon acid, base, salt solvation.

In contrast, the hydroxide OH^- in KOH solution forms a tetrahedron its own with an additional lone

pair (inset e, circled), which forms the O:⇔:O super-HB with one of its four O neighbors. This point compressor has the same, but more significant, effect of mechanical compression on the surrounding O:H-O bond elongation (see Figure 1c). The compressor stiffens the ω_L from below (polarized by K^+) to above 200 cm^{-1} and softens the ω_H as low as 2500 cm^{-1}. The concentration-dependent peak at 3600 cm^{-1} features the H-O bond of the OH^- hydroxide, as shown in Figure 4e and f.

Observations suggest the reason for the burning heat released in the KCl solution. When KCl hydrated, ions soften the ω_H, phonon energy was ejected in the form of Joule heat. Comparing the vibrational spectra of KOH in Figure 3e and of 1.3 GPa pressure in Figure 1c, the effect the poiont compressor of OH^- is much greater than external pressure on the O:H-O phonon shift. From the perspective of polarized charge, the O^{2-}:⇔:O^{2-} repulsive force is four times that of the $H^+ \leftrightarrow H^+$($2^2/1^2$ = 4 times). Capable of fragilization, the point breaker of H^+ lowers the skin stress of the acid HB network but the point compressor and polarizer raise the solution skin stress,[61] as compared in Figure 1b.

As shown in Table 1, H^+ in acid solution forms anti-HBs which causes fragilization of the acid and destruct the surface tension. Although the H-O covalent bond contracts locally in the anti-HB, in the neighboring network of the anti-HB, the O:H bonds were compressed while H-O bonds were lengthened. Oppositely, in salt and alkaline solution, in the HB network, the H-O bonds contract while O:H nonbonds extend, i.e. polarization occurs. Hence, the polarization of H-O:H bond enhance the skin stress while the depolarization of H-O:H network and H^+ fragilization destruct the skin stress.

3.3 Bond stiffness versus surface stress

Integration of the DPS phonon abundance gain as a function of molecular concentration, shown in Figure 5, is the fraction of bonds being conditioned by the solutes. Best fitting of these curves turns out the relationships given in

Table 2. Discussed also the indication of the functional dependence. Derivatives further confirm that the H^+ proton forms the stable H_3O^+ without the ability of polarization but forms the anti-HB

destroying the surface tension. The OH^- tetrahedron forms the O:⇔:O super-HB to compress the O:H-O bonds in the matrix with red-shifting of the H-O bonds to frequencies below 3100 cm^{-1} and meanwhile the H-O bonds of the HO^+ hydroxide possesses the stiffened features of 3610 cm^{-1} for the dangling H-O bonds at water surface.

Table 2. Concentration dependence of the transformation of bonds being conditioned by solutes in HCl, KCl, and KOH solutions.

solution	coefficient	expression	indication
HCl	f_H	0	H_3O^+ formation
KCl	f_K	a[1-exp(-c/b)]	K^+ polarization
HCl &KCl	f_{Cl}		Cl^- polarization & Cl^- - Cl^- correlation
KOH	f_{stiff} (3600 cm^{-1})	0. 9132c	H-O bond of HO^+
	f_{soft} (<3100 cm^{-1})	0. 3597c	O:⇔:O compression

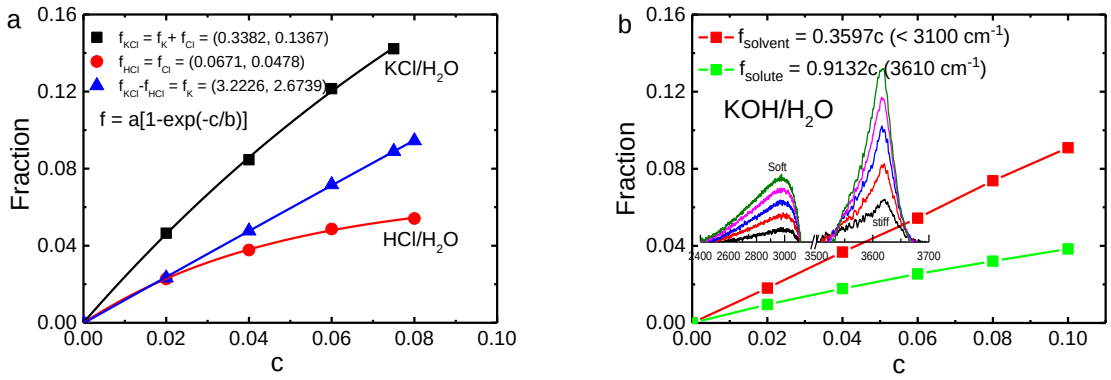

Figure 5. Concentration dependence of the transformation coefficient for (a) K^+, Cl^- in KCl and HCl and for (b) OH^- in KOH solutions with f_{solute} denoting the peak centered at 3610 cm^{-1} and s_{olvent} the feature below 3100 cm^{-1} and f_{loss} the sum of both. The $f_H = 0$ because of the anti-HB formation being not capable of polarization.

4. Conclusions

As a powerful tool, the DPS distills transformation of the stiffness, fraction, and fluctuation of bonds being polarized by ions in HCl and KOH solution or compressed by the O:⇔:O super-HB in KCl solutions, which is beyond the scope of available approaches. The relaxation of the O:H-O bonds in the network caused by H^+, OH^-, K^+ and Cl^- can thus be discriminated as follows:

1) H_3O^+ hydronium formation in acid solution creates the H↔H anti-HB that serves as a point breaker, which is responsible for the skin stress destruction of acid solutions.
2) OH^- hydroxide forms the O:⇔:O super-HB point compressor to soften the H-O bond releasing heat at solvation.
3) K^+ and Cl^- serve each as a point polarizer that aligns, stretches, and polarizes the surrounding O:H-O bonds and makes the hydration shell supersolidity.
4) The DPS also clarifies the fraction coefficients of solutes conditioning the hydrogen bond in the hydration networks.

We have thus verified the presence of quantum switchers (super-HB or anti-HB) and their capabilities of resolving the solute-solvent-solvent interactions and the surface stress of the aqueous solutions, which may extend to general understanding of the solvation process of acids, bases, and salts according to their abilities of creating the excessive H^+ protons, lone pairs, and the ionic polarizers when they are hydrated. The nonbonding fragilization, compression, and polarization shall be critical to the hydration-networks that functionalize DNA, proteins, cells, drugs, and ionic channels, etc.

METHODS

Raman measurements of 150 μL deionised water and aqueous solutions injected into a silica stage were conducted using the confocal micro Raman spectrometer (Renishaw inVia) with a 532-nm He–Ne laser as the light source. To avoid evaporation, the stage was covered with a thin silica lid. The measurements were conducted at the ambient pressure and 298 K temperature. The phonon frequency range was set to 50–4000 cm^{-1}. Each spectrum is an accumulation of four scans, and each scan took 30 seconds. A 50× long-working-distance objective (Leica) was used to focus laser light

onto the sample and collect the scatted light. Signal was detected by a thermoelectric cooled (-70 ºC) standard charge-coupled array detector.

High purity (< 90%) acids, bases, and salts were purchased from Aladdin Co. Deionized water (18.2 MΩ•cm resistivity) produced by a HITECH laboratory water purification system was used for all the measurement.

Acknowledgement

Financial supports from National Natural Science Foundation (No. 11502223) of China, Guangdong Natural Science Foundation (No. 2016A030310060; 2015KQNCX144) and Shenzhen (No. 827000131) are gratefully acknowledged.

References

[1] P. Jungwirth, P.S. Cremer, Nature chemistry, 6 (2014) 261-263.
[2] C.M. Johnson, S. Baldelli, Chemical reviews, 114 (2014) 8416-8446.
[3] P. Lo Nostro, B.W. Ninham, Chemical reviews, 112 (2012) 2286-2322.
[4] J. Ostmeyer, S. Chakrapani, A.C. Pan, E. Perozo, B. Roux, Nature, 501 (2013) 121-124.
[5] J. Kim, D. Won, B. Sung, W. Jhe, The Journal of Physical Chemistry Letters, (2014) 737-742.
[6] M. van der Linden, B.O. Conchúir, E. Spigone, A. Niranjan, A. Zaccone, P. Cicuta, The Journal of Physical Chemistry Letters, (2015) 2881-2887.
[7] W.J. Xie, Y.Q. Gao, The Journal of Physical Chemistry Letters, (2013) 4247-4252.
[8] S. Arrhenius, Nobel Lecture, (1903).
[9] J. Brönsted, Transactions of the Faraday Society, 24 (1928) 630-640.
[10] T.M. Lowry, I.J. Faulkner, Journal of the Chemical Society, Transactions, 127 (1925) 2883-2887.
[11] G.N. Lewis, Journal of the Franklin Institute, 226 (1938) 293-313.
[12] Y.R. Shen, V. Ostroverkhov, Chemical reviews, 106 (2006) 1140-1154.
[13] H. Chen, W. Gan, B.-h. Wu, D. Wu, Y. Guo, H.-f. Wang, The Journal of Physical Chemistry B, 109 (2005) 8053-8063.
[14] M.E. Tuckerman, D. Marx, M. Parrinello, Nature, 417 (2002) 925-929.
[15] S.T. van der Post, C.S. Hsieh, M. Okuno, Y. Nagata, H.J. Bakker, M. Bonn, J. Hunger, Nat Commun, 6 (2015) 8384.
[16] F. Hofmeister, Arch. Exp. Pathol. Pharmacol, 24 (1888) 247-260.
[17] W.M. Cox, J.H. Wolfenden, Proc Roy Soc London A, 145 (1934) 475-488.
[18] P. Ball, J.E. Hallsworth, Physical chemistry chemical physics : PCCP, 17 (2015) 8297-8305.
[19] K.D. Collins, M.W. Washabaugh, Quarterly Reviews of Biophysics, 18 (1985) 323-422.
[20] K.D. Collins, Biophysical chemistry, 167 (2012) 43-59.
[21] K.D. Collins, Biophysical Journal, 72 (1997) 65-76.
[22] X. Liu, H. Li, R. Li, D. Xie, J. Ni, L. Wu, Scientific reports, 4 (2014).
[23] H. Zhao, D. Huang, PLoS ONE, 6 (2011) e19923.

[24] W.B. O'Dell, D.C. Baker, S.E. McLain, PLoS ONE, 7 (2012) e45311.
[25] J.D. Smith, R.J. Saykally, P.L. Geissler, Journal of America Chemical Society, 129 (2007) 13847-13856.
[26] X. Zhang, T. Yan, Y. Huang, Z. Ma, X. Liu, B. Zou, C.Q. Sun, PCCP, 16 (2014) 24666-24671.
[27] Y. Gong, Y. Zhou, H. Wu, D. Wu, Y. Huang, C.Q. Sun, Journal of Raman Spectroscopy, 47 (2016) 1351–1359.
[28] Y. Zhou, Y. Huang, Z. Ma, Y. Gong, X. Zhang, Y. Sun, C.Q. Sun, Journal of Molecular Liquids, 221 (2016) 788-797.
[29] S. Park, M.D. Fayer, Proc Natl Acad Sci U S A, 104 (2007) 16731-16738.
[30] R. Yuan, C. Yan, A. Tamimi, M.D. Fayer, The Journal of Physical Chemistry B, 119 (2015) 13407-13415.
[31] C. de Grotthuss, Galvanique. Ann. Chim, (1806).
[32] A.E. Stearn, H. Eyring, The Journal of Chemical Physics, 5 (1937) 113-124.
[33] G. Wannier, Annalen der Physik, 416 (1935) 545-568.
[34] M.L. Huggins, The Journal of Physical Chemistry, 40 (1936) 723-731.
[35] M. Eigen, Angewandte Chemie International Edition in English, 3 (1964) 1-19.
[36] G. Zundel, P. Schuster, G. Zundel, C. Sandorfy, Recent developments in theory and experiments, 2 (1976).
[37] D. Marx, M.E. Tuckerman, J. Hutter, M. Parrinello, Nature, 397 (1999) 601-604.
[38] C. Drechsel-Grau, D. Marx, Physical Chemistry Chemical Physics, 19 (2017) 2623-2635.
[39] A. Mandal, A. Tokmakoff, The Journal of chemical physics, 143 (2015) 194501.
[40] A. Mandal, K. Ramasesha, L. De Marco, A. Tokmakoff, J Chem Phys, 140 (2014) 204508.
[41] Y. Zhou, D. Wu, Y. Gong, Z. Ma, Y. Huang, X. Zhang, C.Q. Sun, Journal of Molecular Liquids, 223 (2016) 1277-1283.
[42] C. Chaudhuri, Y.-S. Wang, J. Jiang, Y. Lee, H.-C. Chang, G. Niedner-Schatteburg, Molecular Physics, 99 (2001) 1161-1173.
[43] Q. Zeng, T. Yan, K. Wang, Y. Gong, Y. Zhou, Y. Huang, C.Q. Sun, B. Zou, Physical Chemistry Chemical Physics, 18 (2016) 14046-14054.
[44] X. Zhang, Y. Zhou, Y. Gong, Y. Huang, C. Sun, Chem. Phys. Lett., 678 (2017) 233-240.
[45] Editorial, Science, 309 (2005) 78-102.
[46] C.Q. Sun, Y. Sun, The Attribute of Water: Single Notion, Multiple Myths, Springer-Verlag, Heidelberg, 2016.
[47] Y. Huang, X. Zhang, Z. Ma, Y. Zhou, W. Zheng, J. Zhou, C.Q. Sun, Coordination Chemistry Reviews, 285 (2015) 109-165.
[48] C.Q. Sun, in, United States, 2017.
[49] X.J. Liu, M.L. Bo, X. Zhang, L.T. Li, Y.G. Nie, H. TIan, Y. Sun, S. Xu, Y. Wang, W. Zheng, C.Q. Sun, Chemical reviews, 115 (2015) 6746-6810.
[50] J.G. Davis, K.P. Gierszal, P. Wang, D. Ben-Amotz, Nature, 491 (2012) 582-585.
[51] Y.L. Huang, X. Zhang, Z.S. Ma, Y.C. Zhou, W.T. Zheng, J. Zhou, C.Q. Sun, Coordination Chemistry Reviews, 285 (2015) 109-165.
[52] J. Guo, X. Meng, J. Chen, J. Peng, J. Sheng, X.-Z. Li, L. Xu, J.-R. Shi, E. Wang, Y. Jiang, Nat Mater, 13 (2014) 184-189.
[53] Y. Wang, H. Liu, J. Lv, L. Zhu, H. Wang, Y. Ma, Nature communications, 2 (2011) 563.
[54] M. Benoit, D. Marx, M. Parrinello, Nature, 392 (1998) 258-261.
[55] C.Q. Sun, X. Zhang, J. Zhou, Y. Huang, Y. Zhou, W. Zheng, Journal of Physical Chemistry Letters, 4 (2013) 2565-2570.
[56] T.F. Kahan, J.P. Reid, D.J. Donaldson, Journal of Physical Chemistry A, 111 (2007) 11006-11012.
[57] X. Meng, J. Guo, J. Peng, J. Chen, Z. Wang, J.-R. Shi, X.-Z. Li, E.-G. Wang, Y. Jiang, Nature Physics, 11 (2015) 235-239.
[58] J. Guo, J.-T. Lü, Y. Feng, J. Chen, J. Peng, Z. Lin, X. Meng, Z. Wang, X.-Z. Li, E.-G. Wang, Y. Jiang, Science, 352

(2016) 321-325.
[59] P. Cotterill, Progress in Materials Science, 9 (1961) 205-301.
[60] C.Q. Sun, Relaxation of the Chemical Bond, Springer-Verlag, Heidelberg, 2014.
[61] L.M. Levering, M.R. Sierra-Hernández, H.C. Allen, Journal of Physical Chemistry C, 111 (2007) 8814-8826.